
Evaluation of SPECT Angular Sampling Effects: Continuous Versus Step-and-Shoot Acquisition

John A. Bieszk and Eric G. Hawman

Siemens Gammasonics, Inc., Applied Research Group, Des Plaines, Illinois

In order to understand the angular dependence of reconstructed images, a "hot rod" phantom was simulated with six rod sizes ranging from 12.7 mm to 4.8 mm, arranged in 60° sectors. This simulation was used to evaluate changes caused by increasing the number of views from 60 to 180 and to compare results to published angular sampling requirements. Also, a comparison was made of step-and-shoot and continuous data acquisition modes.

Experimental phantom data were taken for three acquisition modes and for two levels of image statistics and compared with the simulation. This study shows the effects of angular aliasing and that image quality generally improves with increasing views even if total image counts are reduced. Despite smoothing effects, a continuous (180 view) scan is, in most cases, the preferred acquisition mode because it offers the highest angular sampling, as well as maximum counting efficiency.

J Nucl Med 28:1308-1314, 1987

As the use of gamma camera emission computed tomographic (ECT) systems grows, people will be looking for guidelines in performing ECT studies. Some pointers have been discussed in the literature concerning the avoidance of artifacts in ECT (1-3) and on the conduction of ECT scans (4,5). Angular sampling and streak artifacts also have been studied (1,6-13). However, requirements such as how many views and how many counts per view are generally uncertain for a particular study. These questions have led to this study of angular sampling in ECT images. We intend to show that an image with more counts may not be a better image than one taken with fewer counts but with better angular sampling.

In the present study, a hot rod phantom was simulated to evaluate the changes caused by increasing the number of views from 60 to 180. To compare different acquisition modes, a model of the deadtime for the step-and-shoot scanning was formulated. Continuous acquisition was simulated by taking each view as a composite of a number of views at closely spaced angular substeps. The phantom was reconstructed for fixed study times. The trade-off of reducing angular

views to improve image statistics was examined as well as a comparison of continuous scans to the step-and-shoot options for two different scan times. These simulations were compared to actual scans of a hot rod phantom* for two distinct count densities. This comparison allowed an evaluation of the simulation predictions as well as a comparison of the trade-offs and benefits in actual scans. Parts of this investigation have been reported previously (14).

METHODS

Phantom Details

A hot rod phantom was simulated with six rod diameters (12.7, 11.1, 9.5, 7.9, 6.4, and 4.8 mm) arranged in 60° sectors. The spacing between the rods is equal to the diameter of the rods. Projections were calculated for a linear sampling of 128 pixels at 3.2 mm/pixel. The effects of Poisson noise (15) and an attenuating water medium were included. Ideal pencil-beam resolution was assumed.

The reader should note that this type of image was chosen to be studied because it would demonstrate aliasing artifacts. The aliasing effects start at the image periphery, where the sampling is coarsest, and move toward the image center as the number of views decreases. A low frequency background was not included because it would contribute little to the intensity of the aliasing artifacts, but would reduce image contrast and hence the visibility of the artifacts.

Received July 23, 1985; revision accepted Feb. 4, 1987.

For reprints contact: John A. Bieszk, Siemens Gammasonics, Inc., Applied Research Group, 2000 Nuclear Dr., Des Plaines, IL 60018.

Reconstruction Details

All reconstructions were done using a filtered backprojection algorithm with a ramp reconstruction filter unless stated otherwise. Since the reconstruction filter affects the spatial frequencies of the data, the results of this work are filter dependent. A ramp filter maximizes spatial detail, but at the cost of maximizing image noise as well. Smoother reconstruction filters reduce the image noise and the potential for aliasing, but at the cost of spatial resolution and contrast (13). An evaluation of the effects of smoother filters is presented in the results section.

Step-and-Shoot Deadtime Model

In step-and-shoot mode, deadtime occurs because acquisition stops while the camera moves from angle to angle. More angular views means more deadtime, hence less counts, for a constant study time. Various ECT systems have different deadtimes. To evaluate deadtime influences, we assumed a simple, representative, deadtime model which utilizes a two speed gantry motion. Each step $\Delta\theta$ consists of a fast movement at rate ω_1 followed by a slower movement at rate ω_2 over a fixed arc α . Hence, the deadtime per step is given by the equation:

$$\tau = \frac{(\Delta\theta - \alpha)}{\omega_1} + \frac{\alpha}{\omega_2} \quad (1)$$

Our simulations have used the following values: $\alpha = 1$ deg, $\omega_1 = 2$ deg/sec, and $\omega_2 = 0.33$ deg/sec.

Continuous Scans

It is assumed that continuous scans have no deadtime and are acquired with 180 angular views. In this study, each view of the simulated continuous mode was the sum of four $1/2$ -degree-increment step-and-shoot projections. This averaging produced a smoothing effect in the data, as expected in true continuous mode. Experimental continuous scans were performed on ECT systems with true continuous motion (i.e., constant angular speed) during acquisition.

Phantom Measurements

The phantom was filled with technetium-99m and a 20% energy window was used. An ultra-high resolution (UHR) collimator and a radius of rotation of ~ 14 cm were used to maximize spatial resolution. Both low and high count studies were performed to compare experimental results to the simulation predictions. Each set of scans was taken sequentially with scan time adjusted for isotope decay.

Calculations of Angular Sampling Requirements

Several studies have given formulas for determining the angular sampling of a scan. Calculations are given below to indicate optimum angular sampling and to use these limits as references with which to evaluate the images showing angular sampling effects in this paper.

Phelps (11), Budinger et al. (6), and Brooks et al. (8) have determined the number of angles for a scan as:

$$N = \frac{\pi D}{2\Delta x} = \text{no. angular samples over } 180^\circ, \quad (2)$$

where D = diameter of object to be scanned
 Δx = linear sampling distance.

Here $\Delta x = 3.2$ mm pixels and $D = 21.6$ cm,

hence $N = 106$ views, giving an angular sampling interval of 1.7°

Joseph and Schulz (10) indicate that for parallel-beam reconstructions over a 180° angular range, the number of angles is given by:

$$N = 2\pi R v_m, \quad (3)$$

where R = radius of "streak"-free reconstruction
 v_m = maximum spatial frequency present in reconstructed images.

The above relations can be used to evaluate the number of views needed to reconstruct an object with certain spatial frequencies. Equation (3) can be used to determine the radius at which streak artifacts begin to occur in a particular image for a given angular sampling rate (Further details on streak artifacts and their object dependence are given in Ref. 10). For the hot rod phantom:

$$R = 10.8 \text{ cm}$$

$$v_m \approx \frac{1}{2d} = 1.04 \text{ cycles/cm for the minimum rod diameter of } 0.48 \text{ cm,}$$

therefore, $N = 71$ views over 180° or 142 views over 360° .

Hence, for $N < 142$ views over 360° , artifacts will exist to some extent in the phantom image. Equations (2) and (3) indicate a large number of angular samples for the imaging of this phantom. However, this work shows that some reduction of this requirement is possible without severely degrading image quality.

RESULTS

Number of Counts Needed to See Simulated Phantom Details

The phantom was simulated with 180 angular views having Poisson noise to determine approximately what intensity was required to see the various details of the phantom. Results of the calculations are shown in Figure 1(A-D) and indicate that $\sim 250k$ counts or more are needed to see the phantom details clearly. (Significantly more counts will be required to see phantom details in images with poorer reconstructed resolution (16).)

The Dependence of Image Quality on the Number of Views

The count level of Figure 1A, 1×10^6 , was chosen to show angular sampling effects on contrast and accuracy of reproduction for a constant image intensity having minimal Poisson noise effects. Figure 2(A-E) shows a degradation of resolution, visibility of central phantom detail, and the increase in streaking artifacts with the decrease in the number of angular views. The 180 view image reproduces rod circularity slightly better than the 120 view image (see the 7.9 mm rods at 10 o'clock), but Figure 2B is very close to Figure 2A in quality. Compared to Figure 2A and 2B, Figure 2C shows some

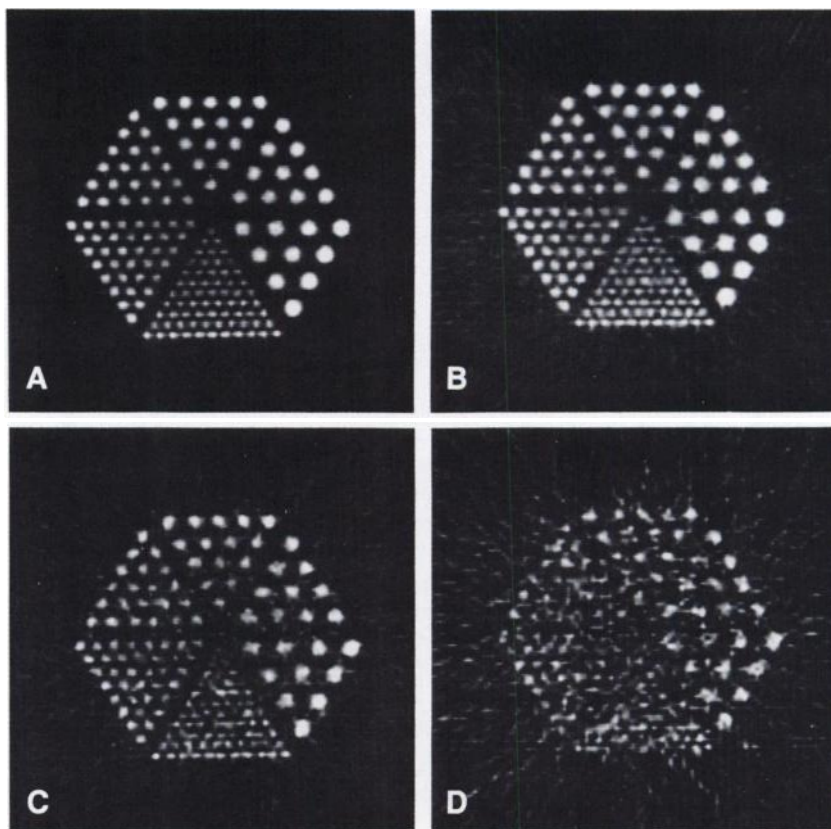


FIGURE 1
Hot rod phantom simulated with 180° views for: A:1M counts, B:250 k counts, C:60 k counts, and D:16 k counts. The 4.8 mm rod section is the bottom (or 6 o'clock) sector of the phantom image. Going clockwise, the next sections are the 6.4, 7.9, 9.5, 11.1, and 12.7 mm rods, respectively.

additional rod distortion and increased aliasing (streaking) in the image periphery. For 60 views (Fig. 2D), the aliasing has invaded the phantom part of the image and introduced artifacts. These appear as the additional modulation of the intensity of the 4.8 mm rods (“streaks”), as well as further distortions of the circular shape of the rods (e.g., see the 11.1 mm sector at 2 o'clock). (Note that these effects may be worse for larger objects or for objects closer to the edge of the field of view, where the sampling is coarsest.) At 30 views, the image is so distorted as to be unrecognizable.

It appears that Figure 2A is the best image, with Figure 2B being a very close second. Considering the 360°-scan predictions of Eqs. (2) and (3) of 212 and 142 views, respectively, the quality of the 120 view image is somewhat surprising.

The greatest improvement in image quality occurs at a low number of views, while only slight improvements occur in going from 120 to 180 views. This result suggests that adequate angular sampling for this image is in this angular range and is consistent with Eq. (3). Generally, objects extending to the edge of the field of view need more views. Also, image quality does not vary strongly with the number of views once the sampling requirements given by Eq. (3) are reached.

Comparison of Simulated Acquisitions

The count level of Figure 1B, 2.5×10^5 , was chosen to demonstrate image changes due to different acquisi-

tion mode choices since statistical effects appear in, but do not dominate, this image, as is the case in Figure 1C and 1D. Figure 3 presents the results of acquisition options for 30- and 60-min scans with attenuation and Poisson noise included. Figures 3A and 3C show that the visibility of the phantom interior and the accurate reproduction of rod shape increase with increasing angular views. Note that for Figure 3C, increasing the number of views actually means decreasing the total counts (Table 1). Furthermore, Figure 3A shows the aliasing effects seen in Figure 2D.

Figure 3 also shows that an awareness of the angular sampling requirements of an object may produce a better reconstructed image in a shorter time. As an example, Figures 3C and 3B show the effects of doubling the angular sampling versus doubling the image statistics of Figure 3A. Note the improvement in visibility of central phantom detail and in circularity of the rods as well as the lack of artifacts in Figure 3C.

A concern about continuous acquisition has been the loss of resolution caused by the camera motion. This simulation predicts only a small change in spatial resolution, due to the continuous camera motion. This change is best seen in the high-count images, Figures 3D and 3F, comparing 120-view step-and-shoot to continuous mode. For shorter scans, when sensitivity may be most important, the continuous acquisition is preferred because of: (a) a large number of angular views (180), and (b) the greatest counting efficiency, and

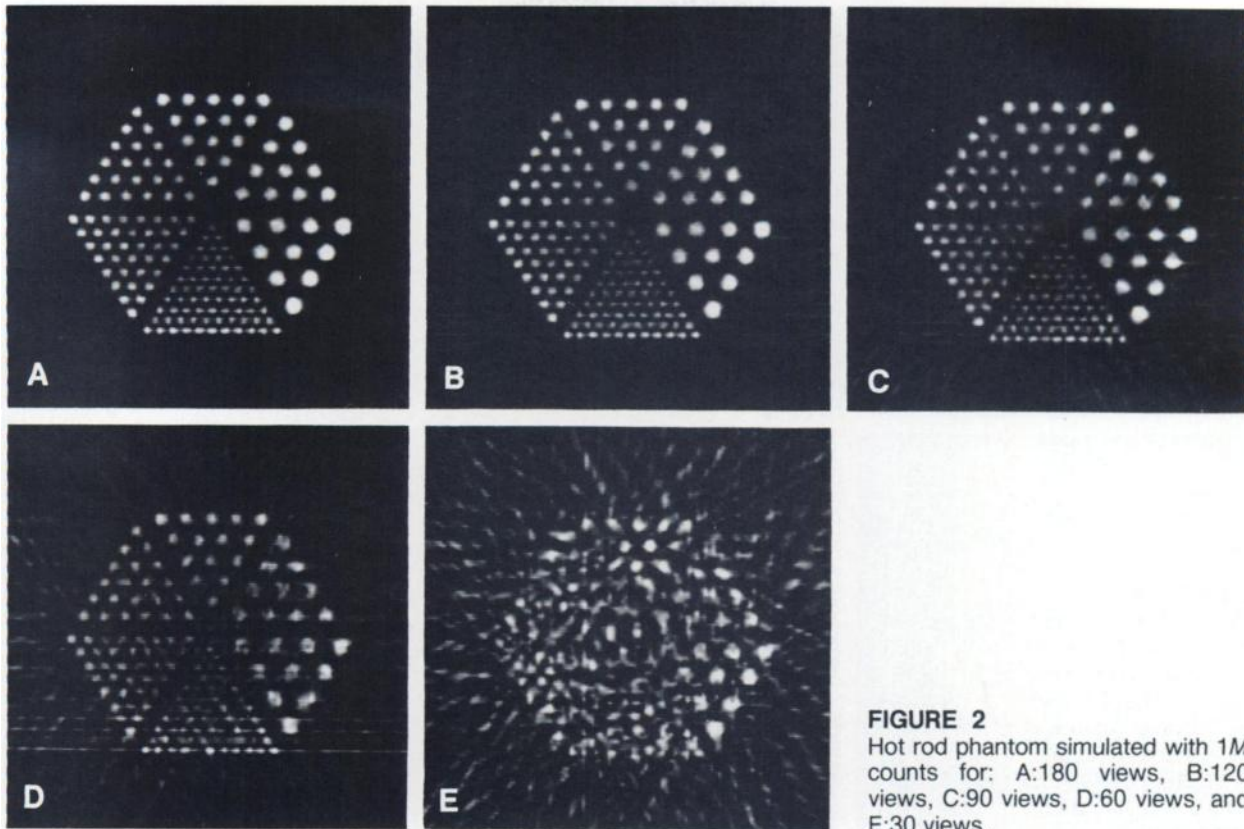


FIGURE 2
Hot rod phantom simulated with 1M counts for: A:180 views, B:120 views, C:90 views, D:60 views, and E:30 views.

hence, best signal-to-noise for a fixed scan time. For longer or phantom scans, where sensitivity is not most important, step-and-shoot modes may well be preferred over continuous mode for better spatial resolution.

Comparison to Experiment

Figure 4 presents the results of the experimental phantom scans. (Details about the images are given in Table 2.) The 60-view studies (Figs. 4A and 4B) show aliasing effects in the streaking artifacts and in rod-shape distortions. Figure 4C shows that reproduction of phantom details improves substantially as the number of views increases from 60 to 120, even though Figure 4C has ~80% of the counts of Figure 4A.

Figures 4C and 4E appear quite similar. Image 4C has better contrast in the 7.9 mm (10 o'clock) sector, but also has more rod distortions (i.e., fewer circular rods). Image 4E better visualizes the first few rows of 6.4 mm rods (the 8 o'clock sector), and has reduced image noise. These reasons lead us to believe that Figure 4E is the best overall short-scan image. Since the 4A, 4C, and 4E scans were acquired for the same study time, the continuous mode appears best, giving the most information without aliasing or artifacts.

The high-count continuous (4F) and the SS 120 (4D) images are quite similar. The rods are generally well-reproduced, with several rows of rods visible in the 6.4 mm section. There is a loss of resolution in the contin-

uous image due to camera motion, but it is a small effect, as one can see. The reader should recall that these studies were done with an UHR collimator and a 14-cm scan radius. Figures 4D and 4F, probably represent the maximum differences in resolution caused by camera motion for 180-view scans. Resolution differences should be even smaller for scans performed at a larger radius of rotation or with a poorer resolution collimator.

Reconstruction Filters

At this point, we shall consider the effects of smoother reconstruction filters. The ramp filter used in the previous images maximizes spatial detail but at the cost of maximizing noise effects as well. Smoother filters will affect aliasing, image signal-to-noise, and image contrast. Figure 5 shows the high-count scans of Figure 4 reconstructed with a Shepp-Logan-Hanning† filter with a cutoff frequency at the Nyquist frequency (SLH1) and the same filter with the cutoff equal to half the Nyquist frequency (SLH2).

The images filtered with SLH1 demonstrate improved signal-to-noise but reduced contrast compared to Figures 4B, 4D, and 4F. Note that aliasing effects in Figure 5A still exist in the 4.8 and 6.4 mm rod sectors, and the use of this filter has cost almost another rod sector in spatial resolution.

The use of a SLH2 filter has almost entirely removed

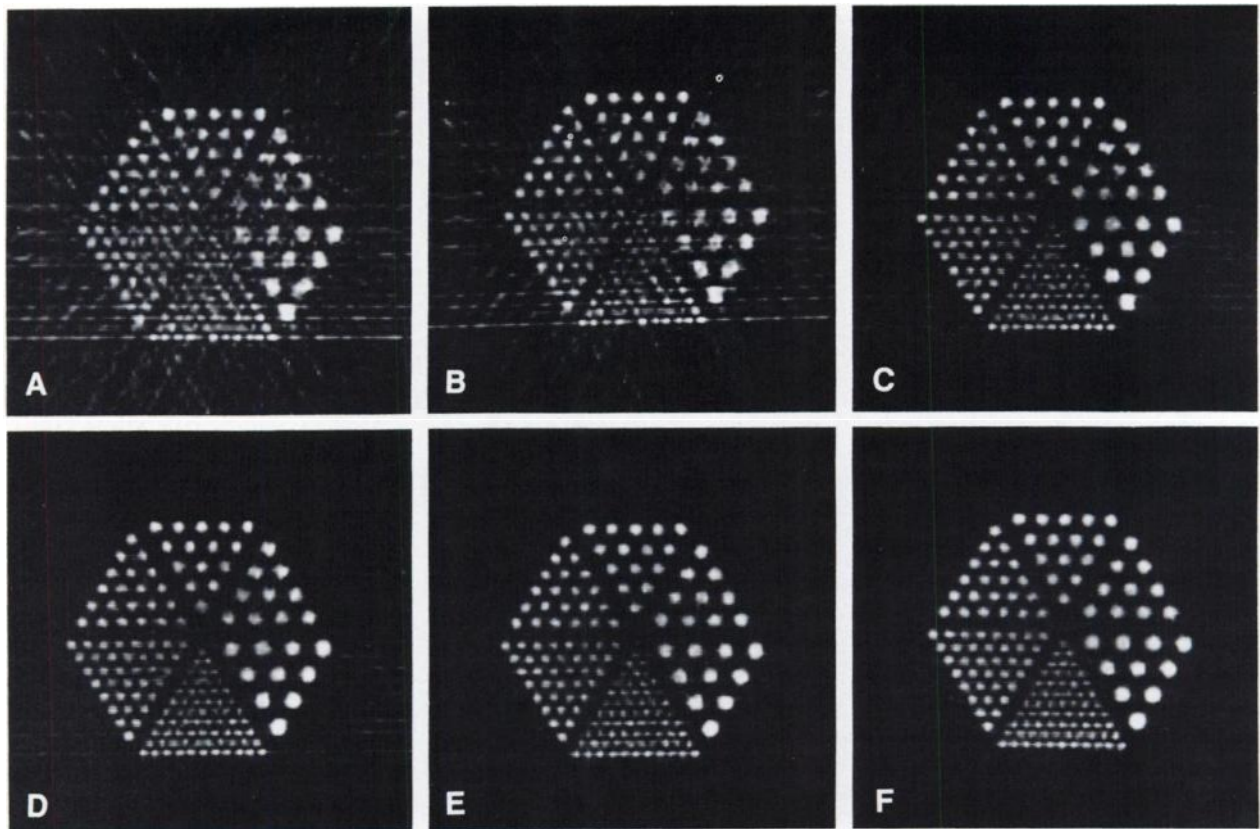


FIGURE 3
A comparison of simulated scans having a constant study time but with different acquisition options (For details see Table 1).

the aliasing artifacts in Figure 5B. Figures 5B, 5D, and 5F appear very similar now, but at a cost in spatial resolution of almost two more sectors over the SLH1 filter and almost three rod sectors over the ramp filter. Figure 5 shows that the choice of reconstruction filter heavily effects the image quality of the reconstructions and will reduce aliasing artifacts but at a cost of spatial resolution and image contrast.

SUMMARY AND CONCLUSIONS

The present study has evaluated angular sampling for the case of a hot rod phantom both by computer simulation and by a series of experimental scans.

Calculations of angular sampling requirements were made from published works. This study has shown that a somewhat reduced number of views can still yield a reconstruction of reasonable image quality.

Our computer simulation indicates that image quality improves with increasing angular views. The greatest improvements occur at a low number of views (e.g., from 60 to 90 views) with the removal of aliasing artifacts and improved accuracy in image fidelity. Decreasing improvements occur with increasing angular sampling, until adequate sampling is reached. Recon-

struction filters can also reduce aliasing artifacts, but at the expense of spatial resolution and image contrast.

Several acquisition modes were evaluated for their statistical and angular sampling trade-offs. This work found that, despite smoothing effects, a continuous (180 view) scan is the preferred acquisition mode in most cases. This mode offers the highest angular sampling, as well as the maximum counting efficiency. For high spatial resolution, high count phantom studies, step-and-shoot acquisitions may be preferred to avoid a

TABLE 1
A Comparison of Image Statistics for Simulated Scans

Nominal scan time	Mode—No. views	Image intensity (k cts)	Figure
30 min	C—180	250	3E
	SS—120	184	3C
	SS— 60	205	3A
60 min	C—180	500	3F
	SS—120	434	3D
	SS— 60	455	3B

* Calculated from $\left(1 - \frac{\text{deadtime}}{\text{nominal scan time}}\right) \cdot \text{continuous mode intensity}$.

TABLE 2
A Comparison of Image Statistics for the ECT Acquisition Modes

Nominal scan time	Mode—No. views	Image intensity (M cts)	Figure
20 min	C—180	1.5	4E
	SS—120	0.93	4C
	SS— 60	1.2	4A
40 min	C—180 [†]	4.7	4F
	SS—120	4.0	4D
	SS— 60	4.5	4B

^{99m}Tc, 20% energy window, UHR collimator, scan rad = 13.7 cm.

[†] The continuous scan is the sum of two 20-min scans taken sequentially.

small amount of resolution blurring due to camera motion.

Another option which could have benefits of both continuous and step-and-shoot modes would be a hybrid scan consisting of step-and-shoot acquisition, but with acquisition during the stepping motion. Each projection would then be a sum of a step-and-shoot view

and a continuous view. Since this study has shown that the continuous scan (for 180 views) has only a slight loss of resolution, this option should have the sensitivity of continuous mode, but with resolution approaching that of step-and-shoot acquisitions.

NOTES

* SPECT Phantom, from Data Spectrum Corporation, 2307 Honeysuckle Road, Chapel Hill, NC.

[†] Reference 13 compares the frequency responses of the filters used in this work. The form of the Shepp-Logan-Hanning filter is:

H(f)

$$= \begin{cases} |f| \cdot \frac{\sin(\pi a f)}{\pi a f} \cdot \frac{1 + \cos\left(\frac{\pi f}{f_c}\right)}{2}, & |f| \leq \min\left(\frac{1}{2a}, f_c\right) \\ 0 & , |f| > \min\left(\frac{1}{2a}, f_c\right) \end{cases}$$

where a = sampling interval
f_c = cutoff frequency.

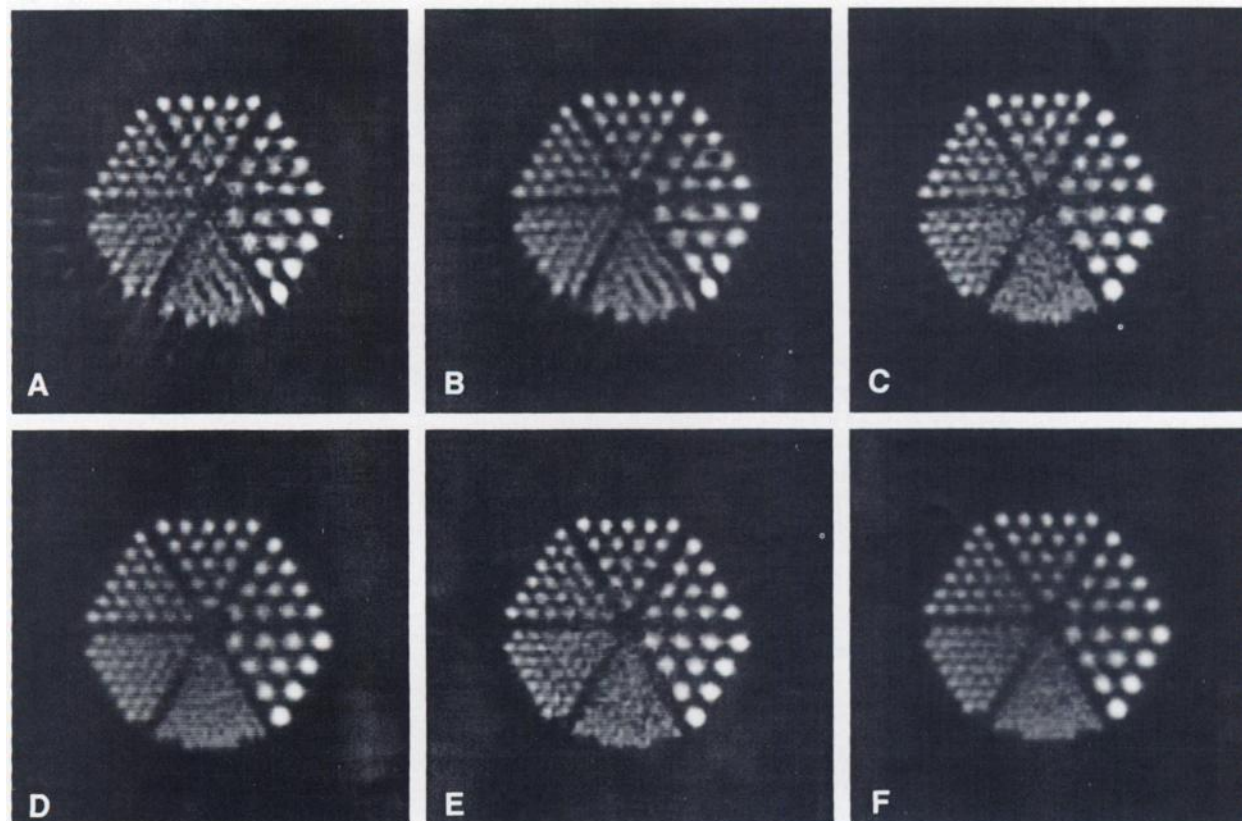


FIGURE 4
A comparison of experimental scans having a constant study time but with different acquisition options. For details about each image see Table 2.

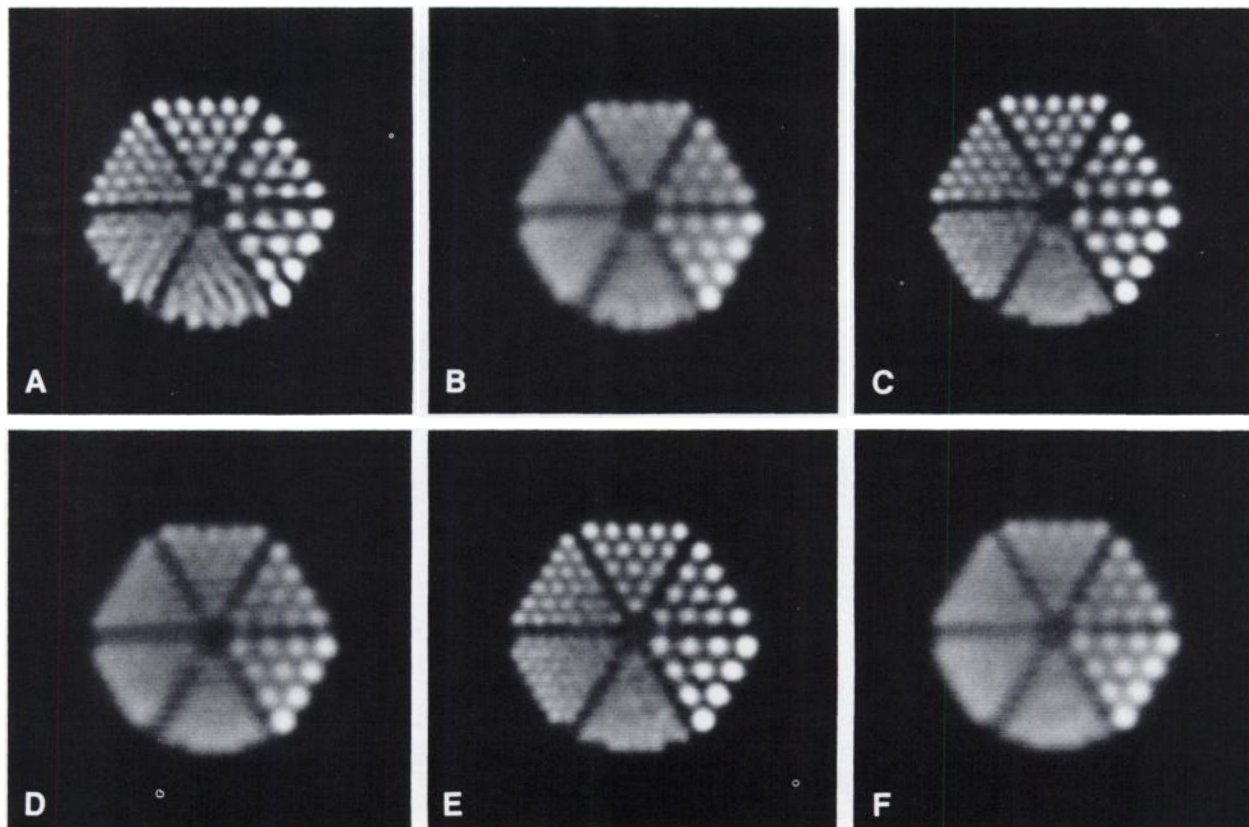


FIGURE 5

The high-count experimental data of Figure 4 reconstructed with the SLH1 filter for: A:SS60, C:SS120, and E:Continuous mode, and with the SLH2 filter for: B:SS60, D:SS120, and F:Continuous mode.

REFERENCES

1. Jaszczak RJ, Coleman RE, Lim CB. SPECT: single photon emission computed tomography. *IEEE Trans Nucl Sci* 1980; NS-27:1137.
2. Williams DL, Ritchie JL, Harp GD, et al. Functional mapping of organ systems and other computer topics. In: Esser P D, ed. *Proceeding of Eleventh Annual Symposium on the Sharing of Computer Programs and Technology in Nuclear Medicine*. New York: The Society of Nuclear Medicine, 149-166, 1981.
3. Rogers WL, Clinthorne NH, Harkness BA, et al. Field-of-view requirements for emission computed tomography with an Anger camera. *J Nucl Med* 1982; 23:162.
4. Greer KL, Coleman RE, Jaszczak RJ. SPECT: a practical guide for users. *J Nucl Med Tech* 1982; 11:61.
5. Harkness BA, Rodgers WL, Clinthorne NH, et al. SPECT: quality control procedures and artifact identification. *J Nucl Med Tech* 1982; 11:55.
6. Budinger TF, Derenzo SE, Gullberg GT, et al. Emission computer assisted tomography with single-photon and positron annihilation photon emitters. *J Comput Assist Tomogr* 1977; 1:131.
7. Shepp LA, Stein JA. Simulated reconstruction artifacts in computerized x-ray tomography. In: Ter-Pogossian MM et al., eds. *Reconstruction tomography in diagnostic radiology and nuclear medicine*. Baltimore: University Park Press, 1977.
8. Brooks RA, Weiss GH, Talbert AJ. A new approach to interpolation in computed tomography. *J Comput Assist Tomogr* 1978; 2:577.
9. Crawford CR, Kak AC. Aliasing artifacts in computerized tomography. *Appl Optics* 1979; 18:3704.
10. Joseph PM, Schulz RA. View sampling requirements in fan beam computed tomography. *Med Phys* 1980; 1:692.
11. Phelps ME. Emission computed tomography. *Semin Nucl Med* 1977; 1:337.
12. Snyder DL, Cox JR Jr. An overview of reconstruction tomography and limitations imposed by a finite number of projections. In: Ter-Pogossian MM, et al., eds. *Reconstruction tomography in diagnostic radiology and nuclear medicine*. Baltimore: University Park Press, 1977.
13. Gustafson DE. Single photon emission computed tomography. In: Robb RA, ed. *Three-dimensional biomedical imaging, Vol II*. Boca Raton: CRC Press, Inc., 1985.
14. Bieszk JA, Hawman EG. An evaluation of the effects of angular sampling and continuous vs. step and shoot acquisition on ECT images using a simulated hot-rod phantom [Abstract]. *Med Phys* 1984; 11:367.
15. Schaffer HE. Algorithm 369. In: *Collected algorithms from the Association for Computing Machinery, Inc., Vol. II*. Association for Computing Machinery, Inc., 1980.
16. Muehllehner G, Colsher JG, Lewitt RM. A hexagonal bar positron camera: problems and solutions. *IEEE Trans Nuc Sci* 1983; NS-30:652.